Design, tolerancing and alignment of pushbroom imaging spectrometers for high response uniformity

Pantazis Mouroulis,[*a] James J. Shea,[#b] David A. Thomas[**a]
[a] Jet Propulsion Laboratory, California Institute of Technology; [b] Swales Aerospace

ABSTRACT

We present a design and tolerancing approach that permits the achievement of a high degree of spatial and spectral uniformity of response from a pushbroom imaging spectrometer. Such uniformity of response is crucial for the extraction of accurate spectroscopic information from remotely sensed data. The spectrometer system example comprises two independent spectrometer modules covering the 400-2500 nm range, separated through a dichroic mirror. The relative merits of alternative approaches are briefly reviewed before concentrating on the problem of building a flight-worthy system that can approximate its design performance. The tolerancing approach requires simultaneous monitoring of many parameters, and specifically: overall image quality, spectral distortion, spectral MTF variation with field, spatial distortion, spatial MTF variation with wavelength, and slit magnification to within a small fraction of a pixel. It is shown that the wavefront error alone or even supplemented by distortion figures is insufficient for characterizing a system with high response uniformity. Tolerance values on the components and their positioning are primarily guided by the need to achieve the same magnification between the two spectrometer modules, as well as by the interferometric alignment method.

1. INTRODUCTION: THE RESPONSE UNIFORMITY PROBLEM

Pushbroom imaging spectrometer systems are well suited to remote observations from space due to their potential for high signal to noise ratio. However, they can suffer from a number of artifacts that compromise identification of spectral signatures when the target presents spatial and spectral variability. These artifacts arise fundamentally from the fact that a pushbroom spectrometer comprises effectively a large number of separate spectrometers, which, however, are not decoupled but interacting. By contrast, a whiskbroom imaging spectrometer has the spectrum of every spatial point recorded on a single linear photodetector array, careful calibration of which suffices to remove most artifacts. In the terminology used here, a pushbroom spectrometer with perfect spectral and spatial uniformity of response would suffer from no artifacts.

The response uniformity problem has been explained in some detail in ref. 1. Translated in optical terms, the uniformity requirements may be summarized as follows:

1) Spectral non-uniformity components: Spectral distortion ("smile"), spatial variation of the PSF width along the spectral direction.
2) Spatial non-uniformity components: Spatial distortion ("keystone"), spectral variation of the PSF width (or height) along the spatial direction, slit magnification mismatch (if two or more spectrometer modules are used – see below).

The PSF width variation is equivalent to an MTF variation in the corresponding direction. Use of the MTF is often advantageous in terms of ease of computation or software availability.

The desired magnitude of the above errors is a small fraction of a pixel. If the sum of the spectral errors is as little as 1-2% of a pixel bandwidth, the system has essentially perfect spectral uniformity.[2] Similarly, if the sum of the spatial errors is less than 4-8% of the pixel width, the system has essentially perfect spatial uniformity.[1] Such values are possible to achieve at the design stage. However, the challenge confronted here is building a flight-worthy system that can maintain these low levels of error.

It should be evident that the focal plane arrays must also support the above uniformity requirements, or at least a suitable calibration scheme must be devised to account for any focal plane response variation. In addition, if two or more arrays are

[*] Corresponding author: pantazis.mouroulis@jpl.nasa.gov, phone: (818) 393-2599, fax (818) 393-9567, 4800 Oak Grove Drive, MS 306-336, Pasadena, CA 91109. [#] jshea@swales.com, phone: (626) 351-6745, 404 N. Halstead St., Pasadena CA 91107, [**] david.a.thomas@jpl.nasa.gov.

needed in order to cover the entire spectral range of interest, they must be perfectly matched in pixel size and total length along the spatial direction.

2. BASIC DESIGN TRADES

We are concerned here with Earth observations from airborne or space-based platforms in the solar reflected spectrum, roughly 400-2500 nm. The configuration that can provide the maximum response uniformity is in principle a single spectrometer and a single focal plane array (FPA), covering the entire range. This may be achievable in the near future, now that suitable detectors are being developed. For the most part, however, the broad spectral range requires at least two separate FPA's, and we restrict the trade space to this case. Typically, the first FPA will be a Si-based detector covering the range 400-1000 nm (VNIR), and the second will be a HgCdTe array covering the 1000-2500 nm range (SWIR).

There are two basic ways to direct light to two separate FPA's: use a dichroic beamsplitter to separate the two spectral regions, or arrange for two spectrometers to have separate, parallel fields of view. Table 1 shows the relative merits of the various solutions

TABLE 1
ALTERNATIVE SYSTEM CONFIGURATIONS

Field-split (two spectrometers)		**Dichroic (one spectrometer)**		**Dichroic (two spectrometers)**	
Advantages	**Disadvantages**	**Advantages**	**Disadvantages**	**Advantages**	**Disadvantages**
'Seamless' VNIR/SWIR transition	SWIR/VNIR FOV split, platform stability concerns	Most economical system	B/S fabrication, availability, polarization, ripple	Identical VNIR/SWIR FOV	B/S fabrication, availability, polarization, ripple
Maximum grating efficiency	Two spectrometers	Best possible SWIR/VNIR magnification match	Grating efficiency lower overall*	Maximum grating efficiency	Two spectrometers
Spectrometer design simpler	SWIR/VNIR magnification match needs tight tolerances	Identical VNIR/SWIR FOV	Possible packaging problems (focal plane proximity)		SWIR/VNIR magnification match needs tight tolerances
	Requires control of telescope distortion		Spectrometer design harder		Spectrometer design harder

*: Requires grating operating in second order for VNIR. Has side effect of providing double dispersion for VNIR.

3. DESIGN DESCRIPTION AND NOMINAL PERFORMANCE

Chosen for this demonstration was the system with two spectrometers and a dichroic beamsplitter. This shows all the tolerancing trades, including the need for magnification match between the two modules.

The system schematic is shown in Fig. 1. The first element after the slit is the dichroic beamsplitter. The short wavelengths are reflected. Envelope and size constraints forced a less than optimum 50° angle for the beamsplitter. This large angle has a measurable effect on the SWIR spectrometer performance and would have been avoided were it otherwise possible. The spectrometers are of the Offner form.[4-6]

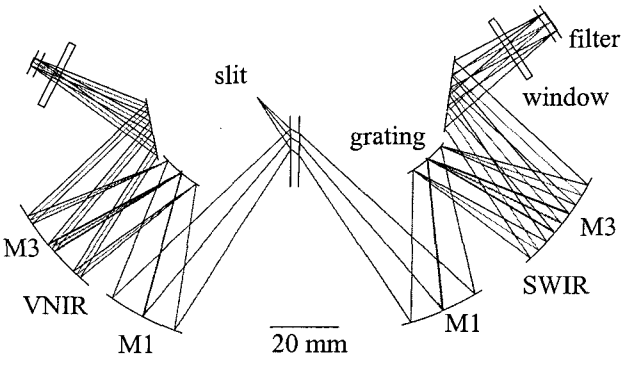

Figure 1. Optical system schematic. The gratings are on the convex surfaces near the fold mirrors. The slit is perpendicular to the paper, so the rays shown coming to a focus represent different wavelengths. There are two windows and two order-rejection filters, the latter being in close proximity to the focal plane arrays (FPAs). All surfaces are spherical or planar. The beamsplitter has a slight wedge to compensate for astigmatism.

This design incorporates the following features: 1) the three spherical surfaces have their apex on a common axis (no tilts or decenters), 2) the two concave mirrors within each module are made concentric, and 3) the mirror curvatures for the VNIR and SWIR modules are identical. These features are important in ensuring that the assembled system will approximate the design performance. Specifically, conditions 1 and 2 facilitate system alignment, while condition 3 helps ensure constant magnification between the two modules. In the latter case, by using the same testplates for the SWIR and VNIR mirrors, similar curvatures can be maintained with an accuracy of about one fringe.

The first order properties of the system are shown in Table 2.

TABLE 2
FIRST-ORDER SPECTROMETER PROPERTIES (NOMINAL VALUES)

Property	Value
Spectral range	400-1000 nm (VNIR)
	900-2500 nm (SWIR)
Magnification	-1
F#	4
Pixel size	27 μm square
Slit length	17.28 mm
Spectral sampling	6.5 nm

The performance of the design is shown in Table 3, which also serves as our recommended way of specifying the optical performance of an imaging spectrometer.

An explanation is necessary about the spectral and spatial response function variation. It has been shown that uncertainty in the halfwidth of the SRF produces an error in the recovered spectra from the target that is approximately one half that of the corresponding error produced by an uncertainty in the peak location of the SRF (smile).[2] The spatial response function variation is assessed through the integrated energy falling on a neighboring pixel (i.e., outside the main pixel). Any variation in that amount of energy as a function of wavelength produces an error similar to keystone.[1]

It is convenient to reduce the number of parameters used to specify the spectral and spatial uniformity. Five such parameters are used in Table 3. We can reduce them to two as follows: 1) We add one half of the SRF variation through field to the smile, and call the resulting number total spectral nonuniformity. In the above example, this amounts to 5.4% for the SWIR and 3.6% for the VNIR. 2) We add the keystone to the SiRF variation and to the magnification mismatch, the latter expressed

as a fraction of a pixel. The resulting numbers are 7.7% for the SWIR and 5.7% for the VNIR. This is the total spatial nonuniformity.

TABLE 3
CALCULATED DESIGN PERFORMANCE

Parameter	VNIR	SWIR
Ensquared energy (27 μm pixel)	97-98% (@400 nm)*	91-93% (@ 900 nm)*
	93-94% (1000 nm)*	81-83% (@ 2500 nm)*
Normalized ensquared energy**	98-99% (@400 nm)	95-97% (@ 900 nm)*
	98-99% (@1000 nm)*	95-98% (@ 2500 nm)*
Smile	0.3 μm (1.1%)	0.5 μm (1.9%)
Keystone	0.6 μm (2.2%)	0.6 μm (2.2%)
SRF halfwidth variation through field ^	5%	7%
SiRF variation through wavelength ~	2%	4%
Magnification mismatch VNIR/SWIR ^^	0.4 μm over full field	0.4 μm over full field
Spatial MTF @Nyquist / diffr. limit#	0.93 / 0.95 (@ 700 nm)	0.83 / 0.85 (@ 1700 nm)
Spectral MTF @Nyquist / diffr. limit#	0.78 / 0.95 (@700 nm)	0.68 / 0.85 (@ 1700 nm)

*: Range shows variation through field
**: Normalized with respect to the ensquared energy for the diffraction-limited PSF.
^: The spectral response function (SRF) is the convolution of the pixel response, the grating response, the slit function, and the optical LSF in the spectral direction (see ref. 1).
~: The spatial response function (SiRF) is the convolution of the pixel response and the optical LSF in the spatial direction (see ref. 1). The spatial response needs to take into account the entire optical system, including the front telescope. In this example, the telescope is ignored.
^^: The magnification is measured at the middle wavelength for each spectrometer. A magnification mismatch number smaller than the keystone value of each spectrometer is not meaningful and can be taken as practically zero.
#: Worst case through field.

It should be clear that the above reduction of parameters is not meant to provide a precise way of representing the total effect, but rather, to provide an easier, although cruder way of monitoring the system performance through tolerancing.

Finally, we should note that similar spectrometer systems can be optimized to provide significantly better response uniformity than the numbers in Table 3 indicate. Most of the performance deterioration can be traced to the 50° beamsplitter angle, which was dictated by packaging constraints, as well as constraints imposed by customer requirements unrelated to optical performance.

4. ALIGNMENT METHOD

The alignment method is critical in producing a system that can approximate its design performance. During the design optimization stage, the primary and tertiary (concave) mirrors are constrained to remain concentric. For the Offner system, this constraint does not result in significant performance degradation. However, it facilitates the alignment significantly. The alignment process starts with making the two concave mirrors concentric, which can be easily and accurately achieved with an interferometer. This reduces the number of degrees of freedom considerably, since the grating is the only remaining powered element in need of alignment. This is typically accomplished by optimizing the image quality to match the expected aberration level at different field points. The alignment aims to achieve not a minimum aberration but a specified aberration. The process has been described in more detail in ref. 3.

Crucial to achieving good results both in the laboratory and in flight is the ability to adjust continuously the mirror position, so as to achieve the necessary fringe-level accuracy. This excludes usual flight-qualified mounts that rely on shims for

changing the spacing or tilt, since such mounts do not provide the necessary accuracy. We use a mounting scheme that combines accuracy and stability by relying on material deformation to provide small movements. This mounting scheme has been developed by Don Moore of JPL.

The mounting scheme permits us to tighten the spacing tolerances to the level of a few microns. Maintaining such small deviations is accomplished by choosing low expansion materials for the bench and mounts, by matching the expansion coefficients between mechanics and optics, and by maintaining a relatively small range of operating temperatures. Although all these mechanical and thermal design trades are important, they are not detailed here since we wish to concentrate on the optics. They are however, critical in ensuring that the tight tolerance values used in the tolerancing procedure are realistic.

The two spectrometers are assembled into a complete system as follows. First, the SWIR spectrometer is assembled interferometrically using a dummy beamsplitter plate, twin to the actual plate except for the dichroic coating so that 633 nm light can be transmitted. This module uses the slit assembly of the final system. Once this module has been assembled and aligned using the procedure described above and in ref. 3, the surrogate beamsplitter plate is replaced with the real one. At this point, verification of the SWIR module performance requires the SWIR focal plane. The VNIR module is also assembled and aligned separately, without the beamsplitter and with a surrogate slit. It is then matched to the SWIR slit by adjustment of the entire module. A small rotation of the beamsplitter about an axis lying in the plane of symmetry of the spectrometer system does not degrade SWIR performance, and may be employed as a final adjustment.

5. TOLERANCING

The goal is to produce a system with total spatial and spectral uniformity at the ~10% pixel level, not much more than the design values noted previously. This requirement in effect includes the image quality specification, since it can only be satisfied if the system stays close to its prescription performance.

The tolerance values shown in the Appendix are necessary in order to achieve the close agreement between design and implementation that we are seeking. The tight tolerance on surface power is justified as follows. Testplates will be generated and their radius measured to the highest accuracy achievable with reasonable effort. With careful polishing, the mirrors may be made to match the testplates to within the tolerance of ±1 fringe shown. However, it is not critical to achieve knowledge of the actual radius to within one fringe. As shown below, the main error is the magnification mismatch between the two spectrometers. But in order to minimize that error, we need only require that the VNIR and SWIR mirrors be identical (within two fringes), which is obtained by making those mirrors to the same testplates. Exact knowledge of the mirror radius is less critical, as small variations from the nominal are in effect automatically compensated for during the interferometric alignment process. This means, however, that the uncertainty in the knowledge of the mirror radius cannot be used as a tolerance value as it would misrepresent the actual performance that can be achieved.

The following additional comments apply to the Table of the Appendix.

1) The beamsplitter surface flatness accounts for deformation from coating stresses.
2) A number of parameters such as glass Abbe number variation or index have negligible impact but were included for completeness.
3) The beamsplitter wedge angle tolerance can be compensated for by a y-tilt, however, that changes the position of the VNIR module significantly. Therefore this compensation was not used.
4) Mirror 1 is taken as a reference surface so it has no tilts or decenters associated with it.
5) The tolerancing process is intended to simulate errors in fabrication, assembly and alignment. Since mirrors M1 and M3 are made concentric to within one-half fringe during alignment, individual spacing tolerances cannot apply to the distances between the powered elements, as they would cause a substantial departure from the concentricity condition, not reflecting the reality of the alignment process. Maintaining the alignment under the conditions of use is, of course, a separate question that needs to be addressed by taking into account a full optomechanical model, with vibration and thermal analysis. Experience with and modeling of our mounting method indicate that the mirrors can be expected to remain stable within a few fringes. Thus a tight tolerance of +/-2 μm applies to the spacings between M1, M3, and grating. That such a tolerance can be achieved during alignment has already been demonstrated.[3] This tolerance can be relaxed by using the distance between grating and M3 to compensate for the distance between M1 and grating, thus effectively ensuring that M1 and M3 remain concentric even when the grating is not positioned exactly.

The optical design software used (ZEMAX, from Focus Software) permits us to establish first the sensitivity of the system to individual errors by assessing the effect of each error separately (sensitivity analysis). The program then reports a number of "worst offenders" and their effect on the merit function. It then generates a random ensemble of perturbed ("Monte Carlo" or MC) systems, in which random error values are combined, based on a statistical distribution chosen by the user (we used a uniform distribution as a somewhat pessimistic case). Since we are attempting to monitor a number of parameters relating to response uniformity that are not evident from the value of the merit function alone, a significant number of the MC perturbed systems must be examined individually.

For ordinary imaging systems, a merit function relating to wavefront error, perhaps augmented by a distortion measure, often suffices to describe the effect of tolerances. In our case, the spectral and spatial uniformity components are a critical part of the merit function. In addition, the system is not designed to achieve the minimum possible wavefront error, but rather, an acceptable level of error, consistent with the best response uniformity condition. A perturbed system may achieve a lower level of wavefront error than the original, but have worse response uniformity. This means that insertion of wavefront error components into the merit function must be done with care, since their minimization does not result necessarily in a better system. For this reason, we originally experimented with a specially constructed merit function that included wavefront error only as deviation from the values of the nominal design. In the end, however, the benefit of this special merit function proved rather small, so the final merit function used for tolerancing was the same as that used during optimization. That merit function contains the default wavefront error components that ZEMAX generates, but their contribution is balanced by the weights applied to the specially inserted uniformity components, as detailed in ref. 1.

5.1 SWIR module

For the first tolerancing run reported below, the back focus was used as compensator and the distance between grating and M3 compensated the change between M1 and grating, as noted before. Table 4 lists the 10 worst offenders, using the parameter tolerance values of the Appendix. MF stands for merit function. The nominal merit function value for the starting design was 0.002235

TABLE 4
WORST OFFENDERS FOR SWIR SPECTROMETER

Parameter	Value (extreme change)*	MF	MF change
M3 radius	1.000000	0.002403	0.000169
M1 radius	-1.000000	0.002365	0.000131
BS y tilt	-0.100000	0.002300	0.000066
BS flatness	1.000000	0.002284	0.000049
DG radius	1.000000	0.002276	0.000041
M3 irregularity	0.500000	0.002275	0.000040
BS wedge	-0.015000	0.002271	0.000036
BS wedge	0.015000	0.002271	0.000036
DG clocking	0.005000	0.002265	0.000030
M1 irregularity	-0.500000	0.002258	0.000023

*: units in this column are the same as in the Appendix

Evidently, the radius tolerance on the primary and tertiary is the main contributor, with two to three times the effect of the next contributor, beamsplitter tilt. The change in the merit function that these tolerance values cause is very small, even for the worst offenders. If image quality (or spot size) was our only concern, the tolerances could be significantly relaxed before any serious deterioration was observed. However, we are interested here in very small and subtle effects, such as distortion or magnification change at the subpixel level.

Summary statistics of 100 MC perturbed systems appear in Table 5. The third column shows the summary statistics of the first forty systems, which can be seen to be similar to those of column 2. This shows that we do not lose much by examining only those forty, which helps reduce the time and effort.

TABLE 5
SUMMARY STATISTICS OF PERTURBED LENSES (SWIR)

	MF value (100 systems)	MF value (40 systems)
Nominal	0.002235	0.002235
Best	0.002201	0.002224
Worst	0.002815	0.002789
Mean	0.002360	0.002371
Standard deviation	0.000126	0.000143
90^{th} percentile	0.002487	0.002511
50^{th} percentile	0.002329	0.002323

The response uniformity computations are too lengthy to be repeated for each of the MC systems. These calculations involve determining the PSFs through field and wavelength, selecting the cases that give the maximum variation, then performing several convolutions with the slit, pixel, and grating functions in order to calculate the spectral and spatial response functions. Even if it were possible to automate this procedure, it would clearly take too long. For this reason, we must seek summary measures of performance that can relate to the expected response uniformity without taking too long to calculate. Such measures will of necessity be empirical and approximate, but they should provide a satisfactory guide about the expected performance. We therefore employ the following simplifications:

1) Based on the observation that the maximum SRF nonuniformity arises from the shortest wavelength, we monitor the change in the spectral MTF for that wavelength only and for two field points that show the maximum MTF difference. We then examine a number of cases to see if an empirical relation can be derived between spectral MTF variation, and SRF variation. It turned out that the MTF difference divided by the MTF sum at the Nyquist frequency (18.5 c/mm) provided good correlation with the SRF halfwidth variation. This was therefore used as a quicker way of estimating spectral nonuniformity due to the SRF width variation.
2) Based on the observation that spatial nonuniformity is caused primarily by the long wavelength PSF spilling out of the pixel due to diffraction, we derive an empirical relation between the sagittal enclosed energy of the most degraded long-wavelength PSF and the spatial nonuniformity, on the assumption that the short wavelength PSF is always sufficiently contained in the pixel. We then monitor only the enclosed energy of a few selected field points at 2500 nm and use that as an indication of spatial nonuniformity. Very good linear correlation was found between x-enclosed energy of the long wavelength PSF and the corresponding induced spatial response function variation. The empirical relation and the fit are shown in Fig. 2.

In addition, the merit function includes smile and keystone components calculated from the chief ray intersections with the image plane. Although the spot centroid, rather than the chief ray, should normally be used, the practical difference between the two in this system has been found to be negligible. It should be noted that random perturbations in the system mean that there is no longer a plane of symmetry. Coupled with potential grating clocking error, this means that the PSF coordinates no longer follow a simple pattern, and finding the difference in x- or y- coordinates is not necessarily a sufficiently accurate characterization of the smile or keystone error. This also excludes the possibility of partial compensation through focal plane rotation or tilt. The numbers derived for smile and keystone of the perturbed systems are therefore approximate, and are likely an overestimate of the true error.

Finally, in order to estimate the magnification difference between the two spectrometers, we monitor the total length of the slit image corresponding to the middle wavelength. Its departure from the nominal is added directly as an equivalent keystone error. This is justified on the basis that we have two spectrometers, each of which can produce a magnification error independent of the other. Only half the magnification difference would be considered as net keystone, because the two focal planes can be aligned about the middle of the field. But since the second spectrometer can also contribute, we take the total deviation from nominal as representing the combined error of both spectrometers. This should provide a reasonably conservative estimate.

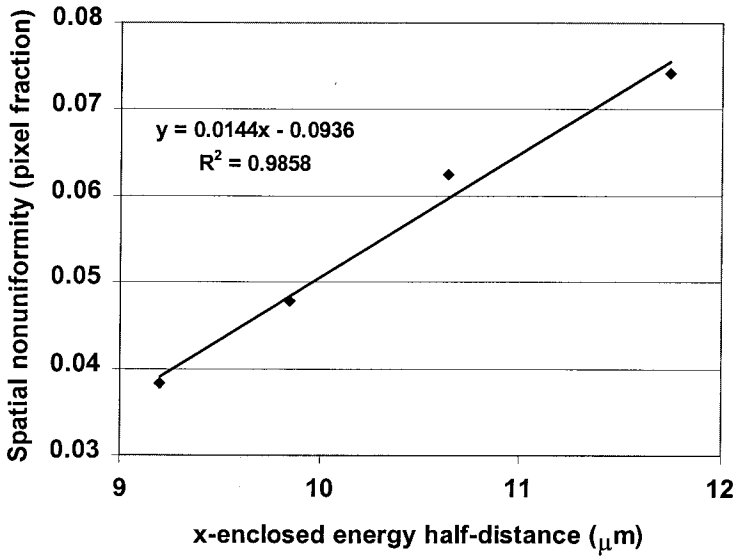

Figure 2: Empirical relation between x-enclosed energy at the 2500 nm wavelength and induced spatial nonuniformity. The abscissa represents the half-distance that encloses 80% of the spot energy in the x-direction.

We select the first forty of the MC systems for a more detailed analysis. The following conclusions emerge:

1) The tight tolerances used mean that the image quality in the spatial direction does not vary by any significant amount. We monitored the sagittal MTF at Nyquist frequency and a wavelength of 1.5 μm. Within all forty systems, the MTF changed between the limits 0.851-0.841, which is negligible and within experimental error. (In the spectral direction, it is more meaningful to speak of the spectral response function in place of image quality – we examine that later). In other words, image quality becomes an essentially irrelevant factor in the tolerancing process.
2) The spatial response function variation component of the total spatial nonuniformity is also practically unaffected by the tolerances. Although there is a contribution of about 4% from the nominal system, the variation imposed by the tolerances is in the range 3.96-4.09%, again entirely negligible.
3) SRF variation is a much more significant contributor to spectral nonuniformity than smile. For example, the mean percentage smile value of all MC systems is 1.5%, whereas the mean spectral nonuniformity is 6.5%, the difference being exclusively due to SRF variation. This cautions strongly against using spectral distortion alone as a measure of spectral uniformity.
4) On average, the proportional contributions to the total spatial nonuniformity are: 20% from keystone, 30% from SiRF variation, and 50% from magnification mismatch, where the latter term accounts for both VNIR and SWIR modules. Even if we consider one spectrometer module in isolation, we see again that specification based on spatial distortion alone would be inadequate.
5) The merit function variation is dominated by the magnification difference in all cases where the merit function is high.

Table 6 shows summary statistics for the spectral and spatial uniformity errors for the first forty MC runs. This Table shows that the dominant error is spatial nonuniformity, caused primarily by slit magnification mismatch. However, the tolerance for spatial nonuniformity can be higher than that for spectral[1], unless the targets of interest are primarily small (pixel-size) or the area to be imaged contains strong spectral and spatial variability. In any case, it is clear from the above that the magnification mismatch is the limiting performance factor in this type of design.

Finally, we examined the effect of compensating the thickness variations between M1 and grating with that between grating and M3 (see operand 10 of Appendix). We allowed those two thicknesses to vary independently by the same ±0.002 mm tolerance as previously, and repeated the tolerance runs. The full results are not shown here, but they can be summarized by saying that the net difference in the as-toleranced system statistics was negligible, although the thickness variations did make the ten worst offender list (Table 4), occupying the rather prominent #4 and #5 spots. Table 7 shows the MC system statistics

for the uncompensated thickness run. Comparison with the first column values of Table 6 shows that there is essentially no difference between the two cases.

TABLE 6
SUMMARY STATISTICS FOR SPECTRAL AND SPATIAL UNIFORMITY ERRORS (SWIR)

	Merit function	Total spectral nonuniformity (pixel fraction)	Spatial nonuniformity, SWIR only (pixel fraction)	Total* spatial nonuniformity (pixel fraction)
Worst	0.002789	0.099	0.114	0.277
Best	0.002224	0.026	0.041	0.048
Mean	0.002371	0.065	0.065	0.133
90th percentile	0.002511	0.079	0.085	0.199
50th percentile	0.002323	0.064	0.065	0.125
Nominal design#	0.002235	0.059	0.063	0.077~

*: includes slit magnification variation
#: The small inconsistency with the values of Section 3 are due to the simplified way of calculating the errors for the MC runs. For consistency, we have recalculated the nominal design values using this less accurate way.
~: For the nominal system, this number is calculated by taking the actual design magnification difference between the two spectrometers. For the toleranced system, the magnification value is necessarily calculated as discrepancy from absolute, which accounts for it being considerably larger than the nominal. But see also Sec. 5.2.

TABLE 7
MC STATISTICS WITH DECOUPLED THICKNESSES

	Merit function
Worst	0.002734
Best	0.002203
Mean	0.002358
90th percentile	0.002535
50th percentile	0.002323

5.2 VNIR module
The reduced diffraction in the VNIR is primarily responsible for the better design performance of the VNIR module, as indicated in Table 3. For the SWIR module, we saw that the SiRF variation was caused by the large amount of diffraction at the long wavelength. This effect is considerably smaller here, as all PSFs are contained well inside the pixel. For this reason, the anticipated SiRF variation is expected to be very small, so it is not monitored in examining the perturbed systems.

The previously established empirical relationship or shortcut for monitoring spectral nonuniformity through the MTF also holds in this case. We follow the same procedure as for the SWIR module and apply the same tolerances, with two exceptions.

1) The tolerance on the distance between beamsplitter and M1 is increased sevenfold to ±0.04 mm. This is because the method of assembly requires us to position the entire spectrometer module relative to an already prepositioned slit and beamsplitter that are part of the SWIR assembly.
2) The tolerance on the y-tilt of the beamsplitter (here simply a mirror), which was not a major concern in the SWIR case, causes an equivalent spectrum rotation at the focal plane. Thus if smile and keystone are measured with respect to the

original x-y coordinate frame, artificially high values result, which overwhelm all other errors by more than an order of magnitude. The $\pm 0.1^{\circ}$ tolerance used earlier causes a shift of tens of μm, when in general we are concerned with values < 1 μm. This effect can be compensated by a simple rotation of the focal plane. Thus, in addition to the rear focal distance, we also allow focal plane rotation and tilt as compensators. But a tighter tolerance of $\pm 0.05^{\circ}$ was still needed.

Table 8 gives the 10 worst offenders for the VNIR module, as Table 4 did for the SWIR.

TABLE 8
WORST OFFENDERS FOR VNIR MODULE

Parameter	Value (extreme change)	units	MF	MF change
BS y-tilt	0.05	degrees	0.003162	0.000031
BS y-tilt	-0.05	degrees	0.003154	0.000023
DG y-decenter	-0.005	mm	0.003147	0.000016
M3 power	-1	fringes	0.003145	0.000014
BS to M1 thick.	-0.04	mm	0.003145	0.000014
M1 power	1	fringes	0.003144	0.000013
DG x-tilt	0.005	degrees	0.003142	0.000011
BS flatness	1	fringes	0.003142	0.000010
DG power	-1	fringes	0.003139	0.000008
M1 irregularity	0.5	fringes	0.003139	0.000008

Clearly, the beamsplitter tilt remains the predominant source of error, even when compensated by the focal plane rotation. However, as the MC analysis will show below, the error is tolerable. In practice, it would be possible to fine tune this tilt to within better than 0.1° with appropriate mounts and without affecting the SWIR, which is more tolerant to this parameter.

We now proceed to analyze the perturbed systems as before. The statistics for 100 MC systems are very similar to the statistics for the first 40, so the first 40 were selected for detailed evaluation. Table 9 shows the results.

TABLE 9
SUMMARY STATISTICS FOR SPECTRAL AND SPATIAL UNIFORMITY ERRORS (VNIR)

	Merit function	Total spectral nonuniformity (pixel fraction)	Spatial nonuniformity, VNIR only (pixel fraction)	Total* spatial nonuniformity (pixel fraction)
Worst	0.003207	0.080	0.142	0.194
Best	0.003127	0.010	0.022	0.035
Mean	0.003151	0.042	0.065	0.114
90th percentile	0.003170	0.071	0.101	0.157
50th percentile	0.003149	0.038	0.057	0.120
Nominal design#	0.003131	0.039	0.057	0.071

*: includes slit magnification variation, but see text below.
#: The small inconsistency with the values of Table 3 are due to the simplified way of calculating the errors for the MC runs. For consistency, we have recalculated the nominal design values using this less accurate way.

Once again it appears that the spatial uniformity is what suffers most. As explained before, the last two columns of Table 9 contain a fixed contribution of 0.02 arising from the SiRF variation. The rest is due to keystone and slit magnification. After subtracting 0.02 from the last two columns and comparing them, we see that in this case the keystone and the slit

magnification contribute approximately equal amounts to the total. There is, however, an additional consideration arising from a detailed look at the magnification results of the MC systems. Specifically, both the SWIR and VNIR perturbed MC systems have a clear tendency to produce a larger than nominal slit. Values under the nominal 17.280 mm occur only in six out of forty MC systems for the SWIR, and nine out of forty for the VNIR. The mean slit length of all forty systems is 17.2814 mm for the SWIR and 17.2809 mm for the VNIR. Therefore, there is some probability that the overall magnification difference between VNIR and SWIR will be less than shown in Tables 6 and 9, where the slit lengths of both the VNIR and the SWIR are subtracted from the nominal individually. Although it is not worth predicting an expected value in detail, this observation gives some additional assurance that the total spatial nonuniformity numbers are quite conservative and would be comfortably met with those tolerances.

The following additional conclusions can be drawn from the analysis of the VNIR perturbed systems.

1) As with the SWIR, the image quality in the sense of spatial MTF is again affected very little by the tolerances. We monitored the sagittal MTF at the Nyquist frequency and 700 nm wavelength, and found it to vary only between 0.922 and 0.907 for all forty systems.
2) As with the SWIR, the smile is the lesser contributor to the total spectral nonuniformity. The SRF variation overwhelms the smile contribution by a factor of about 3:1.
3) Although the slit magnification is a significant overall contributor to the merit function, it is not as dominant as it was for the SWIR case. In some cases, it is keystone that becomes the dominant contributor, and in a couple of cases it is the SRF variation.

6. CONCLUSIONS

Tolerancing a pushbroom imaging spectrometer for high response uniformity requires the development of methods that go well beyond the traditional image quality considerations. The uniformity requirements are far more stringent than image quality. If tight uniformity specifications are to be satisfied, then the spectrometer cannot stray from the design performance sufficiently to cause substantial deterioration in wavefront error. Therefore, tolerancing methods cannot be based on wavefront error alone, or not even on wavefront error supplemented by distortion measures. It has been shown that the effect of the spectral and spatial response function variation can be more significant than the effect of smile and keystone alone. The solution to this problem is to examine a large number of randomly generated systems with various levels of error combinations.

Empirical methods for easier monitoring of the spatial and spectral response uniformity were developed that should be useful in similar spectrometer design and tolerancing studies. Finally, in the specific case of a dual spectrometer system with a dichroic beamsplitter at the input, it was shown that the magnification variation becomes the primary tolerance driver for the SWIR module and to a lesser extent for the VNIR module.

ACKNOWLEDGMENTS

This research was performed at the Jet Propulsion Laboratory, California Institute of Technology, under a contract with the National Aeronautics and Space Administration.

REFERENCES

1. P. Mouroulis, R. O. Green, and T. G. Chrien: "Design of pushbroom imaging spectrometers for optimum recovery of spectroscopic and spatial information", Appl. Opt. **39**, 2210-2220 (2000)
2. R. O. Green: "Spectral calibration requirement for Earth-looking imaging spectrometers in the solar-reflected spectrum", Appl. Opt. **37**, 683-690 (1998)
3. P. Mouroulis and M. McKerns: "Pushbroom imaging spectrometer with high spectroscopic data fidelity: experimental demonstration", Opt. Eng. **39**, 808-816 (2000)
4. A. Offner: "Unit power imaging catoptric anastigmat", U.S. Patent No. 3,748,015 (1973)
5. L. Mertz: "Concentric spectrographs", Appl. Opt. **16**, 3122-3124 (1977)
6. D. Kwo, G. Lawrence, and M. Chrisp: "Design of a grating spectrometer from a 1:1 Offner mirror system", in *Current Developments in Optical Engineering II*, R. E. Fischer and W. J. Smith Eds., Proc. SPIE **818**, 275-278 (1987)

APPENDIX

Tolerance listing for the SWIR spectrometer

Note: BS stands for beamsplitter, DG for diffraction grating.

Number	Parameter	Min	Max	Units
1	Slit/BS spacing	-0.006	0.006	mm
2	BS surface flatness	-1	1	fringes
3	BS thickness	-0.025	0.025	mm
4	BS y-tilt	-0.1	0.1	degrees
5	BS index	-0.001	0.001	
6	BS Abbe #	-0.05	0.05	
7	BS wedge tolerance	-0.015	0.015	degrees
8	BS to M1 spacing	-0.006	0.006	mm
9	M1 radius tolerance	-1	1	fringes
10	M1 to DG to M3 spacing	-0.002	0.002	mm
11	M1 surface irregularity	-0.5	0.5	fringes
12	DG radius tolerance	-1	1	fringes
13	DG X-decenter	-0.005	0.005	mm
14	DG Y-decenter	-0.005	0.005	mm
15	DG X-tilt	-0.005	0.005	degrees
16	DG Y-tilt	-0.005	0.005	degrees
17	DG Z-tilt (clocking)	-0.005	0.005	degrees
18	M3 radius tolerance	-1	1	fringes
19	M3 X-decenter	-0.005	0.005	mm
20	M3 Y-decenter	-0.005	0.005	mm
21	M3 surface irregularity	-0.5	0.5	fringes
22	fold mirror flatness	-0.25	0.25	fringes
23	fold mirror surface irregularity	-0.5	0.5	fringes
24	window flatness	-0.25	0.25	fringes
25	window thickness	-0.0125	0.0125	mm
26	window surface irregularity	-0.25	0.25	fringes
27	window X-tilt	-0.05	0.05	degrees
28	window Y-tilt	-0.05	0.05	degrees
29	window index	-0.001	0.001	
30	window Abbe #	-0.05	0.05	
31	window/filter spacing	-0.0125	0.0125	mm
32	filter flatness	-0.25	0.25	fringes
33	filter thickness	-0.0125	0.0125	mm
34	filter X-tilt	-0.05	0.05	degrees
35	filter Y-tilt	-0.05	0.05	degrees
36	filter index	-0.001	0.001	
37	filter Abbe #	-0.05	0.05	
38	filter surface irregularity	-0.25	0.25	fringes